Sensor-Based Globally Asymptotically Stable Filters for Attitude Estimation: Analysis, Design, and Performance Evaluation

Pedro Batista, *Member, IEEE*, Carlos Silvestre, *Member, IEEE*, and Paulo Oliveira, *Senior Member, IEEE*

***Abstract*—This technical note presents the design, analysis, and performance evaluation of a novel globally asymptotically stable (GAS) filter for attitude estimation. The design is sensor-driven and departs from traditional solutions as no explicit representations of the attitude are considered. The proposed solution yields unique estimates and it does not suffer from drawbacks such as singularities, topological limitations for achieving global stabilization, or unwinding phenomena. The performance of the overall attitude estimation solution is evaluated with the design and implementation of an Attitude and Heading Reference System (AHRS) based on a single low-cost Inertial Measurement Unit. The performance of the proposed AHRS is assessed experimentally using a high precision motion rate table, which provides ground truth signals for comparison with the resulting estimates.**

***Index Terms*—Attitude and heading reference system (AHRS), extended Kalman filters (EKFs), globally asymptotically stable (GAS).**

I. Introduction

The design of Navigation Systems plays a key role in the development of a large variety of mobile platforms. Indeed, the quality of the navigation information is a fundamental requirement in many applications, whether it is for geo-referenced data acquisition purposes or for guidance and control applications. This technical note presents the analysis, design, and performance evaluation of a new class of globally asymptotically stable (GAS) filters for attitude estimation based directly on the aiding sensor measurements.

Traditional attitude estimation methods consist, as discussed in the recent survey paper [1], of a two step process: i) estimate the attitude from body measurements and known reference observations, and ii) filtering the noisy quantities. The first step, where an attitude estimate is obtained from body measurements to feed a filter (or an observer), ends up in one of many known representations [2], e.g., Euler angles, quaternions, Euler angle-axis representation, rotation matrix, etc. For the filtering process there is also a very large number of alternatives, depending on the models and representations of the attitude. Kinematic models, which resort basically to the integration of three-axial rate gyros, are exact. However, these sensors have nonidealities such as biases, which are often time-varying. Dynamic models for the angular velocity, obtained from the simplification of the platform dynamics, are usually complex, highly nonlinear, often time-varying, and the mobile platform inertia matrix and angular damping coefficients may not be well known. With all possible combinations, attitude estimation solutions are many in the literature. Extended Kalman Filters (EKFs) and some other filtering variants have been widely used, see [3] and [4], for instance. In spite of the good performance achieved by EKF and EKF-like solutions, divergence due to the linearization of the system dynamics [1] has led the scientific community to pursue different solutions, in particular nonlinear observers such as those presented in [5] and [6]. For a more thorough survey, the reader is referred to [1]. In all the aforementioned references, sensors data are essentially used to obtain instantaneous measurements of the attitude that are used afterwards to feed a filter or an observer, depending on whether or not a stochastic approach is considered. Sensor specificness is therefore disregarded and, even when it is addressed, the nonlinear transformations that are required to compute the attitude from vector measurements distort noise characteristics. Moreover, with the exception of EKF and EKF-like solutions, systematic tuning procedures are often absent. Exceptions can be found in [7] and [8], where vector measurements are explicitly considered in the design of observers built on the Special Orthogonal Group $SO(3)$ and the Special Euclidean Group $SE(3)$, respectively. In the first, local exponential stability is achieved and the error is shown to converge to zero for almost all initial conditions, while in the second case, almost global exponential stability (AGES) is achieved for the observer error dynamics.

The main contribution of this technical note is the development of a novel class of sensor-based attitude estimation filters that: i) have globally asymptotically stable error dynamics; ii) resort to the angular motion kinematics, which are exact; iii) build on the well-established Kalman filtering theory; iv) provide systematic filter tuning procedures based directly on the sensor noise characteristics, including frequency weights to model colored noise; v) estimate explicitly rate gyro bias and cope well with slowly time-varying bias; and vi) have a complementary structure, fusing low bandwidth vector observations with high bandwidth rate gyro measurements. Most important, the design is sensor-driven and departs from traditional solutions as no explicit representations of the attitude, e.g., Euler angles, quaternions, or rotation matrices, are considered in the filter design. Instead, sensor readings are included directly in the filter dynamics and an attitude representation is obtained afterwards, as in traditional solutions, but using filtered estimates of the sensor measurements. Therefore, the proposed filters yield unique estimates and do not suffer from drawbacks such as singularities, topological limitations for achieving global stabilization, or unwinding phenomena, see [2] and [9].

Essential to the design of the filters is a modification of the nominal sensor-based system dynamics that yields a structure that can be regarded as linear time-varying (LTV), although the system still is, in fact, nonlinear. However, it should be stressed that the resulting system dynamics are exact and no approximations or linearizations are performed whatsoever. For implementation purposes, a Kalman filter is detailed and the final attitude estimation solution results from combining the sensor-based filter with an optimal attitude determination algorithm. This last problem is commonly known in the literature as the Wahba's problem [10]. For two vector observations, there are closed-form solutions available in the literature, see [1], [11], [12], and references therein. Notice that this last step is actually the first step in traditional solutions, which is usually not mentioned as it is often assumed that the attitude, expressed in one of many representations, is available for filtering purposes. Preliminary work by the authors can be found in [13].

This note is organized as follows. The sensor-based framework that is at the core of the proposed solutions is presented in Section II, and,

Manuscript received July 15, 2009; revised November 29, 2010; accepted December 02, 2011. Date of publication February 07, 2012; date of current version July 19, 2012. This work was supported in part by FCT [PEst-OE/EEI/LA0009/2011] and by the EU Project TRIDENT under Contract 248497. Recommended by Associate Editor B. Ninness.

P. Batista and P. Oliveira are with the Institute for Systems and Robotics, Instituto Superior Técnico, Universidade Técnica de Lisboa, Lisboa 1049-001, Portugal (e-mail: pbatista@isr.ist.utl.pt; pjcro@isr.ist.utl.pt).

C. Silvestre was with the Institute for Systems and Robotics, Instituto Superior Técnico, Universidade Técnica de Lisboa, Lisboa 1049-001, Portugal and is now with the Faculty of Science and Technology, University of Macau, Taipa, Macau, China (e-mail: cjs@isr.ist.utl.pt).

Color versions of one or more of the figures in this technical note are available online at http://ieeexplore.ieee.org.

Digital Object Identifier 10.1109/TAC.2012.2187142

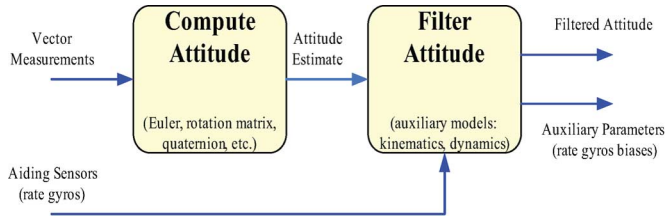

Fig. 1. Classic attitude estimation solution.

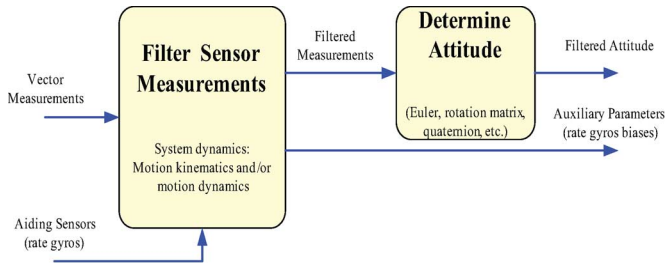

Fig. 2. Sensor-based attitude estimation approach.

in Section III, the observability properties of the resulting system are derived. The filter design and overall structure of the Attitude Determination System (ADS) are detailed in Section IV, whereas experimental results are shown and discussed in Section V. Finally, the main contributions and conclusions are summarized in Section VI.

A. Notation

Throughout this technical note the symbol $\mathbf{0}$ denotes a matrix (or vector) of zeros and $\mathbf{I}$ an identity matrix, both of appropriate dimensions. A block diagonal matrix is represented as $\mathrm{diag}(\mathbf{A}_1, \ldots, \mathbf{A}_n)$. For $\mathbf{x} \in \mathbb{R}^3$ and $\mathbf{y} \in \mathbb{R}^3$, $\mathbf{x} \times \mathbf{y}$ represents the cross product. Finally, the Dirac delta function is denoted by $\delta(t)$ and the magnetic field unit of measurement Gauss is abbreviated as G.

II. Sensor-Based Framework

A. Sensor-Based Concept

The traditional design of attitude filters or observers assumes that instantaneous attitude measurements are readily available for filtering design purposes, which resorts to one of the many attitude representations. Fig. 1 depicts such a solution. As it is possible to observe, vector measurements such as the gravitational and magnetic fields are first used to compute a representation of the attitude of the vehicle. Afterwards, the attitude filter evolves according to the representation of the attitude and resorting to kinematic or dynamic attitude models. With this classic approach the transformations that are necessary to obtain an attitude representation distort the noise characteristics of the sensors. Moreover, attitude representations such as Euler angles, quaternions, rotation matrices, etc., exhibit strong pitfalls such as singularities, topological limitations for achieving global stabilization, or unwinding phenomena, see [2] and [9] for further details. The core concept of the technical note is to take into account the specificness of each sensor by designing the filter directly in the space of the sensors, as exemplified in Fig. 2. An attitude representation, for example a rotation matrix, which does not have singularities and is unique, is then obtained from the filtered estimates. In addition to the inclusion of the specificness of the sensors in the filter design, topological restrictions on $SO(3)$ for achieving global asymptotic stability are no longer in place since the filtering process occurs prior to the determination of the attitude. Furthermore, the proposed solutions do not exhibit any unwinding behaviors.

B. Problem Statement

Let $\{I\}$ denote a local inertial frame, $\{B\}$ the body-fixed frame, and $\mathbf{R}(t) \in SO(3)$ the rotation matrix from $\{B\}$ to $\{I\}$. The attitude kinematics are given by $\dot{\mathbf{R}}(t) = \mathbf{R}(t)\mathbf{S}[\boldsymbol{\omega}(t)]$, where $\boldsymbol{\omega}(t) \in \mathbb{R}^3$ is the angular velocity of $\{B\}$, expressed in $\{B\}$, and $\mathbf{S}(\boldsymbol{x})$ is the skew-symmetric matrix such that $\mathbf{S}(\boldsymbol{x})\boldsymbol{y} = \boldsymbol{x} \times \boldsymbol{y}$. Suppose that there are available vector measurements $\mathbf{y}_1(t) \in \mathbb{R}^3$ and $\mathbf{y}_2(t) \in \mathbb{R}^3$, both expressed in body-fixed coordinates, of known constant vectors in inertial coordinates, i.e., ${}^I\mathbf{y}_1 = \mathbf{R}(t)\mathbf{y}_1(t)$ and ${}^I\mathbf{y}_2 = \mathbf{R}(t)\mathbf{y}_2(t)$, respectively. The reader is referred to [7] for the concept of vector observations and corresponding examples. Then, the dynamics of $\mathbf{y}_1(t)$ and $\mathbf{y}_2(t)$ are given by $\dot{\mathbf{y}}_1(t) = -\mathbf{S}[\boldsymbol{\omega}(t)]\mathbf{y}_1(t)$ and $\dot{\mathbf{y}}_2(t) = -\mathbf{S}[\boldsymbol{\omega}(t)]\mathbf{y}_2(t)$, respectively. Further consider rate gyro measurements $\boldsymbol{\omega}_m(t) \in \mathbb{R}^3$ corrupted with bias $\mathbf{b}_{\boldsymbol{\omega}} \in \mathbb{R}^3$, i.e. $\boldsymbol{\omega}_m(t) = \boldsymbol{\omega}(t) + \mathbf{b}_{\boldsymbol{\omega}}(t)$. Then, the sensor-based system dynamics are given by

$$\begin{cases} \dot{\mathbf{x}}_1(t) = -\mathbf{S}\left[\boldsymbol{\omega}_m(t)\right]\mathbf{x}_1(t) + \mathbf{S}\left[\mathbf{b}_{\boldsymbol{\omega}}(t)\right]\mathbf{x}_1(t) \\ \dot{\mathbf{x}}_2(t) = -\mathbf{S}\left[\boldsymbol{\omega}_m(t)\right]\mathbf{x}_2(t) + \mathbf{S}\left[\mathbf{b}_{\boldsymbol{\omega}}(t)\right]\mathbf{x}_2(t) \\ \dot{\mathbf{b}}_{\boldsymbol{\omega}}(t) = \mathbf{0} \\ \mathbf{y}_1(t) = \mathbf{x}_1(t) \\ \mathbf{y}_2(t) = \mathbf{x}_2(t) \end{cases}. \tag{1}$$

The problem considered here is the design of a filter solution for the nominal nonlinear system (1), considering also additive system disturbances and sensor noise. Notice that, once filtered estimates of $\mathbf{x}_1(t)$ and $\mathbf{x}_2(t)$ are obtained, the attitude can be immediately computed using classic methods.

III. Observability Analysis

The observability of the nonlinear system (1) is examined in this section. To that purpose, notice that using the cross product property $\boldsymbol{x} \times \boldsymbol{y} = -\boldsymbol{y} \times \boldsymbol{x}$, it is possible to rewrite (1) as

$$\begin{cases} \dot{\boldsymbol{x}}(t) = \mathbf{A}(t)\boldsymbol{x}(t) \\ \mathbf{y}(t) = \mathbf{C}\boldsymbol{x}(t) \end{cases} \tag{2}$$

where

$$\mathbf{A}(t) = \begin{bmatrix} -\mathbf{S}\left[\boldsymbol{\omega}_m(t)\right] & \mathbf{0} & -\mathbf{S}\left[\mathbf{y}_1(t)\right] \\ \mathbf{0} & -\mathbf{S}\left[\boldsymbol{\omega}_m(t)\right] & -\mathbf{S}\left[\mathbf{y}_2(t)\right] \\ \mathbf{0} & \mathbf{0} & \mathbf{0} \end{bmatrix}$$

and

$$\mathbf{C} = \begin{bmatrix} \mathbf{I} & \mathbf{0} & \mathbf{0} \\ \mathbf{0} & \mathbf{I} & \mathbf{0} \end{bmatrix}.$$

Notice that the relations $\mathbf{x}_1 = \mathbf{y}_1$ and $\mathbf{x}_2 = \mathbf{y}_2$ were used in order to write the system matrix $\mathbf{A}(t)$ in such a way that it does not depend on the system state. Indeed, all entries of $\mathbf{A}(t)$ may just be considered as continuous bounded known functions of t. Now, although the system dynamics (2) are nonlinear, they may, nevertheless, be regarded as LTV for observability and observer design purposes, as in the following lemma [14, Lemma 1].

Lemma 1: Consider the nonlinear system

$$\begin{cases} \dot{\mathbf{x}}(t) = \boldsymbol{\mathcal{A}}\left(t, \mathbf{u}(t), \mathbf{y}(t)\right)\mathbf{x}(t) + \boldsymbol{\mathcal{B}}(t)\mathbf{u}(t) \\ \mathbf{y}(t) = \boldsymbol{\mathcal{C}}(t)\mathbf{x}(t) \end{cases}. \tag{3}$$

If the observability Gramian $\boldsymbol{\mathcal{W}}(t_0, t_f)$ associated with the pair $(\boldsymbol{\mathcal{A}}(t, \mathbf{u}(t), \mathbf{y}(t)), \boldsymbol{\mathcal{C}}(t))$ on $\mathcal{I} = [t_0, t_f]$ is invertible then the nonlinear system (3) is observable in the sense that, given the system

input $\{\mathbf{u}(t), t \in \mathcal{I}\}$ and the system output $\{\mathbf{y}(t), t \in \mathcal{I}\}$, the initial condition $\mathbf{x}(t_0)$ is uniquely defined.

Before presenting the main result of this section, the following lemma is introduced, see [15, Proposition 4.2].

Lemma 2: Let $\mathbf{f}(t) : [t_0, t_f] \subset \mathbb{R} \rightarrow \mathbb{R}^n$ be a continuous and two times continuously differentiable function on $\mathcal{I} := [t_0, t_f]$, $T := t_f - t_0 > 0$, and such that $\mathbf{f}(t_0) = \mathbf{0}$. Further assume that $\ddot{\mathbf{f}}(t)$ is bounded on $\mathcal{I}$. If there exists a positive constant α and $t_i \in \mathcal{I}$ such that $\|\dot{\mathbf{f}}(t_i)\| \geq \alpha$, then there also exists a positive constant β and $0 < \delta \leq T$ such that $\|\mathbf{f}(t_0 + \delta)\| \geq \beta$.

The following theorem addresses the observability of (2).

Theorem 1: If the vector observations are non parallel or, equivalently

$$ {}^{I}\mathbf{y}_1 \times {}^{I}\mathbf{y}_2 \neq \mathbf{0} \tag{4}$$

then the pair $(\mathbf{A}(t), \mathbf{C})$ is uniformly completely observable.

Proof: Let $\mathbf{R}_m(t) \in SO(3)$ be a rotation matrix such that $\dot{\mathbf{R}}_m(t) = \mathbf{R}_m(t)\mathbf{S}[\boldsymbol{\omega}_m(t)]$ and consider the Lyapunov transformation $\mathbf{z}(t) = \mathbf{T}(t)\boldsymbol{x}(t)$, with $\mathbf{T}(t) := \operatorname{diag}(\mathbf{R}_m(t), \mathbf{R}_m(t), \mathbf{I})$, which preserves observability properties [16]. The new system dynamics are given by $\dot{\mathbf{z}}(t) = \boldsymbol{\mathcal{A}}(t)\mathbf{z}(t), \mathbf{y}(t) = \boldsymbol{\mathcal{C}}(t)\mathbf{z}(t)$, where

$$\boldsymbol{\mathcal{A}}(t) = \begin{bmatrix} \mathbf{0} & \mathbf{0} & -\mathbf{R}_m(t)\mathbf{S}\left[\mathbf{y}_1(t)\right] \\ \mathbf{0} & \mathbf{0} & -\mathbf{R}_m(t)\mathbf{S}\left[\mathbf{y}_2(t)\right] \\ \mathbf{0} & \mathbf{0} & \mathbf{0} \end{bmatrix},$$

$$\boldsymbol{\mathcal{C}}(t) = \begin{bmatrix} \mathbf{R}_m^T(t) & \mathbf{0} & \mathbf{0} \\ \mathbf{0} & \mathbf{R}_m^T(t) & \mathbf{0} \end{bmatrix}$$

and the transition matrix associated with $\boldsymbol{\mathcal{A}}(t)$ is given by

$$\boldsymbol{\phi}(t, t_0) = \begin{bmatrix} \mathbf{I} & \mathbf{0} & -\int_{t_0}^{t} \mathbf{R}_m(\sigma)\mathbf{S}\left[\mathbf{y}_1(\sigma)\right] d\sigma \\ \mathbf{0} & \mathbf{I} & -\int_{t_0}^{t} \mathbf{R}_m(\sigma)\mathbf{S}\left[\mathbf{y}_2(\sigma)\right] d\sigma \\ \mathbf{0} & \mathbf{0} & \mathbf{I} \end{bmatrix}.$$

Let $\mathbf{d} = [\mathbf{d}_1^T \mathbf{d}_2^T \mathbf{d}_3^T]^T \in \mathbb{R}^9$ be a unit vector, with $\mathbf{d}_i \in \mathbb{R}^3$, $i = 1, 2, 3$. If $\boldsymbol{\mathcal{W}}(t_0, t_f)$ denotes the observability Gramian associated with the pair $(\boldsymbol{\mathcal{A}}(t), \boldsymbol{\mathcal{C}}(t))$ on $[t_0, t_f]$, it is a simple matter of computation to show that $\mathbf{d}^T\boldsymbol{\mathcal{W}}(t, t+\delta)\mathbf{d} = \int_t^{t+\delta} \|\mathbf{f}(\tau, t)\|^2 d\tau$ for all $t \geq t_0$, where

$$\mathbf{f}(\tau, t) := \begin{bmatrix} \mathbf{d}_1 - \int_t^{\tau} \mathbf{R}_m(\sigma)\mathbf{S}\left[\mathbf{y}_1(\sigma)\right] \mathbf{d}_3 d\sigma \\ \mathbf{d}_2 - \int_t^{\tau} \mathbf{R}_m(\sigma)\mathbf{S}\left[\mathbf{y}_2(\sigma)\right] \mathbf{d}_3 d\sigma \end{bmatrix}$$

$\tau \in [t, t+\delta], t \geq t_0$. For $\mathbf{d}_1 \neq \mathbf{0}$ or $\mathbf{d}_2 \neq \mathbf{0}$ it is clear that $\|\mathbf{f}(t,t)\| \geq \|\mathbf{d}_1\| = \alpha_1$ or $\|\mathbf{f}(t,t)\| \geq \|\mathbf{d}_2\| = \alpha_2$, respectively, for all $t \geq t_0$. On the other hand, if $\mathbf{d}_1 = \mathbf{d}_2 = \mathbf{0}$, it follows that $\|\mathbf{d}_3\| = 1$, $\mathbf{f}(t,t) = \mathbf{0}$, and

$$\left.\frac{\partial \mathbf{f}}{\partial \tau}(\tau, t)\right|_{\tau=t} = -\begin{bmatrix} \mathbf{R}_m(t)\mathbf{S}\left[\mathbf{y}_1(t)\right] \mathbf{d}_3 \\ \mathbf{R}_m(t)\mathbf{S}\left[\mathbf{y}_2(t)\right] \mathbf{d}_3 \end{bmatrix}.$$

Now, suppose that (4) is true. Then, it is also true that $\mathbf{y}_1(t) \times \mathbf{y}_2(t) \neq \mathbf{0}$ for all $t \geq t_0$ and hence there exists $\alpha_3 > 0$ such that $\|(\partial \mathbf{f}/\partial \tau)(\tau, t)|_{\tau=t}\| \geq \alpha_3$ for all $t \geq t_0$ and $\|\mathbf{d}_3\| = 1$. In addition, notice that the second derivative of $\mathbf{f}$ with respect to τ is bounded on $[t, t+\delta]$, uniformly in t. But this means, using Lemma 2, that there exist $\alpha_4 > 0$ and $\delta_1 > 0$ such that $\|\mathbf{f}(t+\delta_1, t)\| \geq \alpha_4$ for all $t \geq t_0$. Therefore, there exist positive constants α^* and δ^* such that $\|\mathbf{f}(t+\delta^*, t)\| \geq \alpha^*$ for all $t \geq t_0$ and $\mathbf{d} \in \mathbb{R}^9$, $\|\mathbf{d}\| = 1$. But then, using Lemma 2 again, there also exist positive constants α and δ such that $\mathbf{d}^T\boldsymbol{\mathcal{W}}(t, t+\delta)\mathbf{d} \geq \alpha$ for all $t \geq t_0$ and $\mathbf{d} \in \mathbb{R}^9$, $\|\mathbf{d}\| = 1$. This suffices to conclude that the pair $(\mathbf{A}(t), \mathbf{C})$ is uniformly completely observable as both matrices are norm-bounded, which concludes the proof. ∎

This result is fundamental to assess the stability of the Kalman filter that will be presented in Section IV.

Remark 1: Although Theorem 1 provides only a sufficient condition, it is this condition that interests in general for attitude estimation. Indeed, if (4) is not verified, i.e., if the vectors are parallel, the LTV system (2) may still be uniformly completely observable. However, since both vectors are parallel, it is impossible to determine the attitude.

Remark 2: Notice that Theorem 1 provides also a constructive result on the design of state observers for (2). Indeed, if the pair $(\mathbf{A}(t), \mathbf{C})$ is uniformly completely observable, then it is possible to design a linear state observer with globally asymptotically stable error dynamics for the dynamic system (2), following the results of Lemma 1. A similar example of application of this result can be found in [14], where the problems of source localization and navigation based on single range measurements were addressed.

IV. Attitude Determination System

A. Sensor-Based Filter Design

Considering that the underlying system dynamics can be regarded as linear for observability purposes, a natural estimation solution is to use a continuous-time Kalman filter. Considering additive system disturbances and sensor noise, the system dynamics are given by

$$\begin{cases} \dot{\boldsymbol{x}}(t) = \mathbf{A}(t)\boldsymbol{x}(t) + \mathbf{w}(t) \\ \mathbf{y}(t) = \mathbf{C}\boldsymbol{x}(t) + \mathbf{n}(t) \end{cases} \tag{5}$$

where $\mathbf{w}(t) = [\mathbf{w}_1^T(t)\, \mathbf{w}_2^T(t)\, \mathbf{w}_3^T(t)]^T \in \mathbb{R}^9$ is zero-mean white Gaussian noise, with $\mathrm{E}[\mathbf{w}(t)\mathbf{w}^T(t-\tau)] = \boldsymbol{\Xi}\delta(\tau)$, $\mathbf{n}(t) = [\mathbf{n}_1^T(t)\, \mathbf{n}_2^T(t)]^T \in \mathbb{R}^6$ is zero-mean white Gaussian noise, with $\mathrm{E}[\mathbf{n}(t)\mathbf{n}^T(t-\tau)] = \boldsymbol{\Theta}\delta(\tau)$ and $\mathrm{E}[\mathbf{w}(t)\mathbf{n}^T(t-\tau)] = \mathbf{0}$. Notice that, for filter design purposes, both $\mathbf{w}(t)$ and $\mathbf{n}(t)$ could have been modeled as the outputs of stable linear time invariant filters, which could be easily employed to model, e.g., colored noise, see [17] for an example of such application. In this technical note, and for the sake of clarity of presentation, the simplest white Gaussian noise version is presented.

The Kalman filter equations for the system dynamics (5) are standard [18]–[20]. The state estimate evolves according to

$$\dot{\hat{\mathbf{x}}}(t) = \mathbf{A}(t)\hat{\mathbf{x}}(t) + \mathbf{K}(t)\left[\mathbf{y}(t) - \mathbf{C}\hat{\mathbf{x}}(t)\right] \tag{6}$$

where the Kalman gain matrix is given by $\mathbf{K}(t) = \mathbf{P}(t)\mathbf{C}^T\boldsymbol{\Theta}^{-1}$, where $\mathbf{P}(t)$ is the covariance matrix, which satisfies $\dot{\mathbf{P}}(t) = \mathbf{A}(t)\mathbf{P}(t) + \mathbf{P}(t)\mathbf{A}(t) + \boldsymbol{\Xi} - \mathbf{P}(t)\mathbf{C}^T\boldsymbol{\Theta}^{-1}\mathbf{C}\mathbf{P}(t)$.

It is important to stress that the resulting structure is complementary: high bandwidth rate gyro measurements are combined with low frequency vector observations to determine a low frequency disturbance in the gyro measurements and provide filtered estimates of the vector observations, see [7] for details on complementary filtering.

Remark 3: One should notice that additive Gaussian noise may not be the best modeling option. Indeed, multiplicative noise would be more accurate, as the presence of noise in the gyro measurements is reflected as terms like $\mathbf{S}[\mathbf{w}_i(t)]\mathbf{x}_i(t), i = 1, 2$, instead of simple additive system disturbances. Also, different noise distributions could better model the sensors noise. As an alternative, it is possible to consider $\mathbf{w}(t) \in \mathcal{L}_2$ and $\mathbf{n}(t) \in \mathcal{L}_2$, where $\mathcal{L}_2$ denotes the space of square integrable signals, and design an $\mathcal{H}_\infty$ filter instead of a Kalman filter. The steps are similar and therefore will be omitted.

B. ADS Structure

The final Attitude Determination System results from combining the sensor-based filter with an algorithm that determines the proper rotation

matrix $\hat{\mathbf{R}} \in SO(3)$ which best explains the vector estimates provided by the filter. This corresponds to the sensor-based structure depicted in Fig. 2, where the sensor-based filter that yields filtered vector estimates corresponds to the Kalman filter (6) and the attitude is obtained by finding the proper rotation matrix $\hat{\mathbf{R}}(t)$ that minimizes the loss function

$$J\left(\hat{\mathbf{R}}(t)\right) = \frac{1}{2}\sum_{i=1}^{2} a_i \left\|\hat{\mathbf{y}}_i(t) - \hat{\mathbf{R}}^T(t)^I\mathbf{y}_i\right\|^2, a_i > 0, i = 1, 2.$$

This problem is known in the literature as the Wahba's problem [10] and in this technical note the attitude matrix is reconstructed using the closed-loop (and computationally efficient) optimal solution presented in [12]. The coefficients a_i can be chosen to reflect the confidence on each sensor.

Remark 4: There is nothing in the filter structure imposing any particular relation between $\hat{\mathbf{y}}_1(t)$ and $\hat{\mathbf{y}}_2(t)$. Moreover, there are no restrictions on the norms of the vector estimates. In fact, if any of these restrictions was imposed, it would not be possible to achieve globally asymptotically stable error dynamics due to topological limitations, see [9]. Due to the absence of these restrictions, it may happen that, for some time instant t, $\hat{\mathbf{y}}_1(t)$ and $\hat{\mathbf{y}}_2(t)$ are parallel or null. In this case, the optimal solution presented in [12] is not well defined and as such an alternative must be considered. A simple solution is to employ directly the vector measurements when the vector estimates are parallel or null, which yields a unique solution for the rotation matrix.

Remark 5: It is important to stress that the stability properties of the filter are not affected by the issue discussed in the previous remark, as the filter process occurs prior to the determination of the estimate of the rotation matrix. Moreover, in the absence of noise, the error of the estimate of the rotation matrix will always converge to zero, as after the initial transients of the filter fade out, the estimate of the rotation matrix is obtained from the vector estimates, whose error converges to zero. In the presence of sensor noise, the error will naturally remain confined to a neighborhood of the origin.

C. Integration of Additional Attitude Aiding Devices

Although the design presented in the note relies only on two vector observations, the proposed solution is trivially extended for multiple vector observations. Indeed, all that is required is to add more states to the system dynamics (5) and to modify the attitude determination algorithm to cope with more than two vector observations. This is quite useful as there exists a myriad of commercially available sensors that provide vector measurements useful for attitude determination. Notice that in this case the specificness of each sensor can still be directly incorporated in the filter design and colored noise is easily modeled, as opposed to classical solutions that use the vector measurements solely to compute an instantaneous attitude representation used to feed an observer or filter built on one of the many attitude representations.

V. Experimental Evaluation

A. Experimental Setup

In order to evaluate the performance of the proposed sensor-based filter and the resulting Attitude Determination System, an Attitude and Heading Reference System (AHRS), based on a single Inertial Measurement Unit, was designed, implemented, and tested. The IMU contains three sets of orthogonally mounted rate gyros, accelerometers, and magnetometers, therefore providing sufficient vector observations for attitude estimation, along with angular velocity measurements. The IMU that was employed was the NANO IMU NA02-0150F50, from MEMSENSE, which is a low cost sensor that outputs data at a rate of 150 Hz. The worst case standard deviation values provided by the manufacturer are 0.0015 G and 0.008 $\mathrm{m/s^2}$ for the magnetometers and accelerometers, respectively, and $0.95^\circ/\mathrm{s}$ for the rate gyros.

In simulation environment the true values are always available, which allows for an easy evaluation of the performance of the proposed designs. In order to experimentally evaluate the performance of the proposed AHRS, the experiments were carried out with a 3 degree-of-freedom high accuracy Motion Rate Table, Model 2103HT from Ideal Aerosmith. This table has three rotational joints which allow for movement about 3 orthogonally mounted axis, so called inner, middle, and outer axis, and that were defined as the x, y, and z axis of the body-fixed reference frame. Therefore, the rotation from body-fixed coordinates to inertial coordinates can be written as $\mathbf{R}(t) = \mathbf{R}_z(\theta_{out}(t))\mathbf{R}_y(\theta_{mid}(t))\mathbf{R}_x(\theta_{inn}(t))$, where $\mathbf{R}_x(.)$, $\mathbf{R}_y(.)$, and $\mathbf{R}_z(.)$ are the rotation matrices about the x, y, and z axis, respectively, and θ_{inn}, θ_{mid}, and θ_{out} are the inner, middle, and outer axis angles, respectively. The table outputs the angular positions with a resolution of 0.00025°, considered as ground truth signals.

Unfortunately, the motion rate table heavily distorts the magnetic field in the neighborhood of the IMU, even though it was attempted to place the IMU as far as possible from the remaining experimental setup. Therefore, magnetic field measurements were simulated in the loop in real time using the table angular position measurements and realistic sensor noise was added so that the results are as realistic as possible. In practical applications, many sources of magnetic field disturbances can be accounted for calibrating the magnetometer, see [21] and references therein, which makes the magnetometer a common sensor employed in attitude estimation.

B. Performance Evaluation

The real-time performance of the AHRS is assessed in this section. The evolution of the inner, middle, and outer angles is depicted in Fig. 3. Notice that the angular motion full range is used, and if Euler angles were employed problems would have arised due to singularities. Also, although not depicted in the technical note, the angular velocity $\boldsymbol{\omega}(t)$, reaches interesting values. The Kalman filter parameters were set according to the sensor noise levels, $\boldsymbol{\Xi} = 0.5\mathrm{diag}(0.0015\mathbf{I}, 0.008\mathbf{I}, 2 \times 10^{-10}\mathbf{I})$ and $\boldsymbol{\Theta} = \mathrm{diag}(0.0015\mathbf{I}, 0.008\mathbf{I})$. No particular emphasis was given on the tuning process as the resulting performance with these simple parameters is very good. In practice, the spectral contents of the sensors noise may be experimentally approximated and frequency weights adjusted to improve the performance of the filter, see the examples provided in [17]. Moreover, correlation between the system disturbances $\mathbf{w}$ and the sensor noise $\mathbf{n}$ may also be considered. Since $\mathbf{x}_1$ and $\mathbf{x}_2$ are measured, these variables were initialized with the first set of measurements. The initial bias estimate was set to zero.

The initial convergence of the filter errors for the magnetic and gravitational fields is shown in Fig. 4. The filter convergence is extremely fast. Since it is not possible to plot the evolution of the bias error, as the true bias is unknown, Fig. 5 displays the initial convergence of the bias estimate and the detailed evolution after the initial transients fade out. As it can be seen, the rate gyros biases estimates changes over time, which is quite typical of low-cost units.

In order to evaluate the overall attitude performance, yaw, pitch, and roll Euler angles could have been computed from the estimated rotation matrix. However, as these would have singularities due to the full-range trajectory described by the attitude, and for the purpose of performance evaluation only, an additional error variable is defined as $\tilde{\mathbf{R}}(t) = \mathbf{R}^T(t)\hat{\mathbf{R}}(t)$, which corresponds to the rotation matrix error. Using the Euler angle-axis representation for this new error variable

$$\tilde{\mathbf{R}}(t) = \mathbf{I}\cos\left(\tilde{\theta}(t)\right) + \left[1 - \cos\left(\tilde{\theta}(t)\right)\right]\tilde{\mathbf{d}}(t)\tilde{\mathbf{d}}^T(t) - \mathbf{S}\left(\tilde{\mathbf{d}}(t)\right)\sin\left(\tilde{\theta}(t)\right) \quad (7)$$

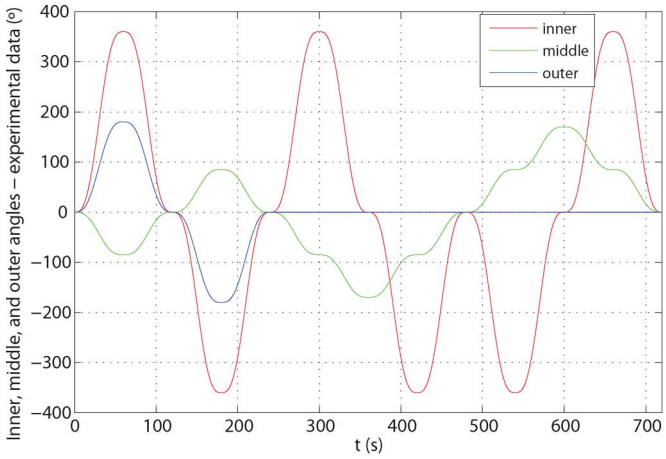

Fig. 3. Evolution of the inner, middle, and outer angles.

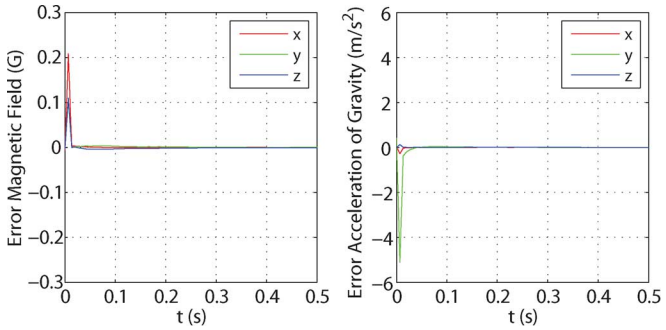

Fig. 4. Initial convergence of the filter error.

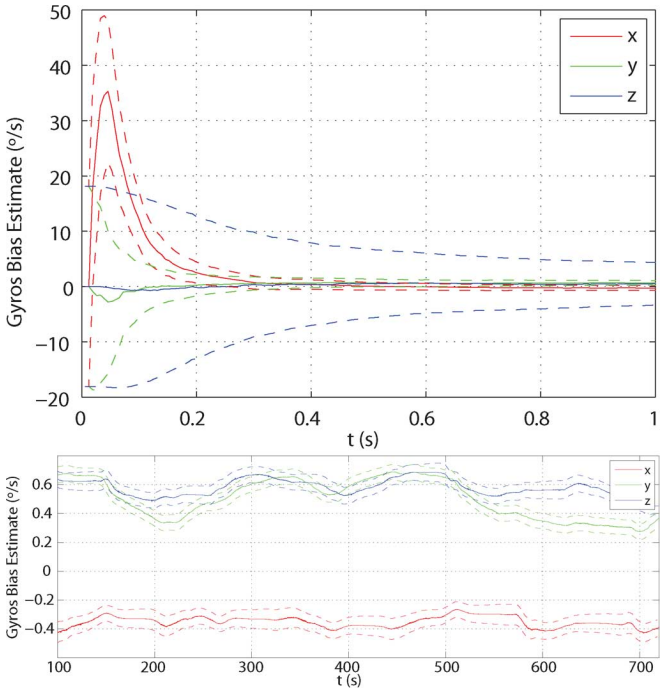

Fig. 5. Evolution of the rate gyros biases estimates ($1-\sigma$ bounds around the estimates are shown using dashed lines).

where $0 \leq \tilde{\theta} \leq \pi$ and $\tilde{\mathbf{d}} \in \mathbb{R}^3, \|\tilde{\mathbf{d}}\| = 1$, are the angle and axis that represent the rotation error, the performance of the filter is easily identified from the evolution of $\tilde{\theta}$. The mean angle error, in steady state (which is achieved in less than 1 s), using the angle-axis representation (7), is 0.125°, which is a very good value considering the low performance specifications of the IMU at hand. It is also comparable with the results obtained in simulation, where the mean error was 0.064° considering that real sensors do not have white Gaussian noise distributions. Further improvements could be achieved by analyzing the spectral contents of the sensor measurements at rest and including the sensor frequency response specifications in the filter design.

VI. Conclusion

Attitude Determination Systems are a critical component for the successful operation of mobile robotic platforms. Although there exists a myriad of solutions in the literature for attitude estimation, these usually have significant pitfalls such as singularities, lack of global asymptotic stability results, or unwinding phenomena. This technical note presented the analysis, design, and performance evaluation of a GAS sensor-based attitude filter. Since the design of the filters does not resort to any specific representation of the attitude, the aforementioned drawbacks do not affect the proposed solutions. The performance of the overall attitude estimation solution was evaluated with the design and implementation of a low-cost Attitude and Heading Reference System based on a single Inertial Measurement Unit. A high precision calibration table, which provided ground truth data for comparison purposes, was employed, and the results were compatible with the simulations that were carried out prior to the experiments. Finally, the results are also particularly good considering the low-grade characteristics of the IMU that was employed.

Acknowledgment

The authors wish to thank B. Cardeira, L. Sebastião, A. Oliveira, and J. Tojeira for their expertise and contributions.

References

[1] J. Crassidis, F. Markley, and Y. Cheng, "Survey of nonlinear attitude estimation methods," *J. Guid., Control Dyn.*, vol. 30, no. 1, pp. 12–28, Jan./Feb. 2007.

[2] M. Shuster, "A survey of attitude representations," *J. Astronaut. Sci.*, vol. 41, no. 4, pp. 439–517, Oct./Dec. 1993.

[3] J. Farrell, "Attitude determination by Kalman filter," *Automatica*, vol. 6, no. 5, pp. 419–430, 1970.

[4] I. Bar-Itzhack and Y. Oshman, "Attitude determination from vector observations: Quaternion estimation," *IEEE Trans. Aerosp. Electron. Syst.*, vol. AES-321, no. 1, pp. 128–136, Jan. 1985.

[5] J. Thienel and R. Sanner, "A coupled nonlinear spacecraft attitude controller and observer with an unknown constant gyro bias and gyro noise," *IEEE Trans. Autom. Control*, vol. 48, no. 11, pp. 2011–2015, Nov. 2003.

[6] H. Rehbinder and B. Ghosh, "Pose estimation using line-based dynamic vision and inertial sensors," *IEEE Trans. Autom. Control*, vol. 48, no. 2, pp. 186–199, Feb. 2003.

[7] R. Mahony, T. Hamel, and J.-M. Pflimlin, "Nonlinear complementary filters on the special orthogonal group," *IEEE Trans. Autom. Control*, vol. 53, no. 5, pp. 1203–1218, Jun. 2008.

[8] J. Vasconcelos, R. Cunha, C. Silvestre, and P. Oliveira, "Landmark based nonlinear observer for rigid body attitude and position estimation," in *Proc. 46th IEEE Conf. Decision Control*, New Orleans, LA, Dec. 2007, pp. 1033–1038.

[9] S. Bhat and D. Bernstein, "A topological obstruction to continuous global stabilization of rotational motion and the unwinding phenomenon," *Syst. Control Lett.*, vol. 39, no. 1, pp. 63–70, 2000.

[10] G. Wahba, "A least squares estimate of spacecraft attitude," *SIAM Rev.*, vol. 7, no. 3, p. 409, Jul. 1965.

[11] M. Shuster and S. Oh, "Three-axis attitude determination from vector observations," *J. Guid., Control Dyn.*, vol. 4, no. 1, pp. 70–77, Jan./Feb. 1981.

[12] F. Markley, "Optimal attitude matrix from two vector measurements," *J. Guid., Control Dyn.*, vol. 31, no. 3, pp. 765–768, May/Jun. 2008.
[13] P. Batista, C. Silvestre, and P. Oliveira, "Sensor-based complementary globally asymptotically stable filters for attitude estimation," in *Proc. 48th IEEE Conf. Decision Control*, Shanghai, China, Dec. 2009, pp. 7563–7568.
[14] P. Batista, C. Silvestre, and P. Oliveira, "Single range aided navigation and source localization: Observability and filter design," *Syst. Control Lett.*, vol. 60, no. 8, pp. 665–673, Aug. 2011.
[15] P. Batista, C. Silvestre, and P. Oliveira, "On the observability of linear motion quantities in navigation systems," *Syst. Control Lett.*, vol. 60, no. 2, pp. 101–110, Feb. 2011.
[16] R. Brockett, *Finite Dimensional Linear Systems*. New York: Wiley, 1970.
[17] P. Batista, C. Silvestre, and P. Oliveira, "Optimal position and velocity navigation filters for autonomous vehicles," *Automatica*, vol. 46, no. 4, pp. 767–774, Apr. 2010.
[18] R. Kalman and R. Bucy, "New results in linear filtering and prediction theory," *Trans. ASME—J. Basic Eng.*, ser. D, vol. 83, no. 3, pp. 95–108, Mar. 1961.
[19] A. Gelb, *Applied Optimal Filtering*. Cambridge, MA: The MIT Press, 1974.
[20] A. Jazwinski, *Stochastic Processes and Filtering Theory*. Waltham, MA: Academic Press, Inc., 1970.
[21] J. Vasconcelos, G. Elkaim, C. Silvestre, P. Oliveira, and B. Cardeira, "A geometric approach to strapdown magnetometer calibration in sensor frame," *IEEE Trans. Aerosp. Electron. Syst.*, vol. 47, no. 2, pp. 1293–1306, Apr. 2011.

Variable Gain Super-Twisting Sliding Mode Control

Tenoch Gonzalez, *Student Member, IEEE*,
Jaime A. Moreno, *Member, IEEE*, and
Leonid Fridman, *Member, IEEE*

***Abstract*—In this note, a novel, Lyapunov-based, variable-gain super-twisting algorithm (STA) is proposed. It ensures for linear time invariant systems the global, finite-time convergence to the desired sliding surface, when the matched perturbations/uncertainties are Lipschitz-continuous functions of time, that are bounded, together with their derivatives, by known functions. The proposed algorithm has similar properties to the variable-gain first-order sliding mode control, but it provides alleviation to the chattering phenomenon. The results are verified experimentally.**

***Index Terms*—Chattering effect, discontinuous systems, Lyapunov functions, robust control, second-order sliding modes.**

I. Introduction

1) Motivation: Sliding mode (SM) control is a well-known tool for rejecting matched uncertainties/disturbances (see [7], [20], [21], for example). Usually the sliding mode control design (see [20], [21, Ch. 5]) consists of two steps:

- Construction of the desired sliding surface;
- SM enforcement.

In the first generations of SM controllers either relay controllers or unit controllers were used ([9], [20], [21]). The main disadvantage of these control strategies is the so-called "chattering effect" (see [20] and [21], for example).

The three main approaches to chattering alleviation and attenuation in SM systems were proposed in the mid-1980's:

- The use of saturation control instead of the discontinuous one [5], [19]. This approach allows for control continuity but cannot restrict the system dynamics onto the switching surface. It only ensures the convergence to a boundary layer of the sliding manifold, whose size is defined by the slope of the saturation characteristics.
- The observer-based approach [4]. This method allows to bypass the plant dynamics by the chattering loop. This approach reduces the problem of robust control to that of exact and robust estimation.

Manuscript received December 09, 2010; revised August 23, 2011; accepted November 17, 2011. Date of publication December 14, 2011; date of current version July 19, 2012. This work was supported by CONACyT (Consejo Nacional de Ciencia y Tecnología) under Grants 51244, 132125, andCVU 208168, FONCICyT 93302; by Programa de Apoyo a Proyectos de Investigación e Innovación Tecnológica (PAPIIT) under UNAM, Grants 117610 and 117211; and by Fondo de Colaboración del II-FI, UNAM, IISGBAS-165-2011. Recommended by Associate Editor A. Ferrara.

T. Gonzalez is with the Programa de Maestría y Doctorado en Ingeniería Eléctrica (control), Universidad Nacional Autónoma de México, UNAM, Coyoacan, 14240, México, Tlalpan D.F., México (e-mail: tenoch@ieee.org).

J. A. Moreno is with the Coordinación de Eléctrica y Computación, Instituto de Ingeniería, Universidad Nacional Autónoma de México, Coyoacán, 04510 México D.F., Mexico (e-mail: JMorenoP@ii.unam.mx; moreno@pumas.iingen.unam.mx).

L. Fridman was with the Departamento de Control Automático, CINVESTAV-IPN, A.P. 14-740, D.F., Mexico. He is now with the Departamento de Ingeniería de Control y Robótica, Engineering, Engineering Faculty, Universidad Nacional Autónoma de México, UNAM, Coyoacan, México D.F., México. (e-mail: lfridman@unam.mx).

Color versions of one or more of the figures in this technical note are available online at http://ieeexplore.ieee.org.

Digital Object Identifier 10.1109/TAC.2011.2179878